ELSEVIER

Journal of Organometallic Chemistry 519 (1996) 229–235

Journal of Organometallic Chemistry

Organometallic complexes for non-linear optics V [1] Syntheses and computationally-derived quadratic non-linearities of *trans*-[Ru(C≡CC$_6$H$_4$R-4)Cl(dppm)$_2$] (R = H, NO$_2$, C$_6$H$_4$NO$_2$-4, CH=CHC$_6$H$_4$NO$_2$-4,(*E*)); X-ray crystal structure of *trans*-[Ru(C≡CC$_6$H$_4$C$_6$H$_4$NO$_2$-4,4′)Cl(dppm)$_2$]

Andrew M. McDonagh [a], Ian R. Whittall [a], Mark G. Humphrey [a,*], Brian W. Skelton [b], Allan H. White [b]

[a] *Department of Chemistry, Australian National University, Canberra, A.C.T. 0200, Australia*
[b] *Department of Chemistry, University of Western Australia, Nedlands, W.A. 6907, Australia*

Received 28 December 1995

Abstract

A series of systematically-varied donor–acceptor octahedral ruthenium σ-acetylide complexes of general formula *trans*-[Ru(C≡CC$_6$H$_4$R-4)Cl(dppm)$_2$] (R = H, NO$_2$, C$_6$H$_4$NO$_2$-4, CH=CHC$_6$H$_4$NO$_2$-4,(*E*)) has been synthesized. An X-ray structural study of *trans*-[Ru(C≡CC$_6$H$_4$C$_6$H$_4$NO$_2$-4,4′)Cl(dppm)$_2$] reveals non-planarity of the biphenylene moiety in the solid state. Semi-empirical calculations employing ZINDO were performed on the acetylide complexes and the dichloro species *cis*- and *trans*-[RuCl$_2$(dppm)$_2$] to evaluate molecular quadratic optical non-linearities, β; the results are consistent with (a) a significant increase in β upon incorporation of a strong acceptor substituent, (b) a substantial increase in β on chain lengthening, and (c) a 50% decrease in non-linearity upon rotation of phenylene–phenylene dihedral angle from coplanarity to orthogonality for the structurally-characterized complex.

Keywords: Ruthenium; Acetylide; Alkynyl; Non-linear optics; Quadratic hyperpolarizabilities; Crystal structure

1. Introduction

The need for new materials with large non-linear optical responses has prompted the investigation of a wide range of possible materials [2]. Studies of organometallic complexes have concentrated on measurements of bulk material second order responses ($\chi^{(2)}$) [3,4], which shed little light on the intrinsic molecular non-linearity, an understanding of which is essential for rational materials design. Kanis et al. have demonstrated that the semi-empirical routine ZINDO accurately reproduces EFISH-derived molecular quadratic hyperpolarizabilities β for ferrocenyl, (arene)chromium tricarbonyl [5,6], (pyridine)tungsten pentacarbonyl [5], and some main group organometallic compounds [7]. We have recently utilized ZINDO to assess the effect of phosphine substitution, M–C(acetylide) bond length variation, and orientation of the acetylide aryl group on second-order non-linearity in some (cyclopentadienyl)bis(phosphine)-ruthenium σ-arylacetylide complexes [8]; although we made no attempt to demonstrate that the computed responses had significance in an absolute sense, studies involving a systematically-varied series of complexes permit comparison in a relative fashion, and extraction of structure–property information.

Octahedral ruthenium acetylide complexes have attracted attention recently, both for their catalytic potential [9,10] and their possible applications in materials science [11–17]. We have now extended our investiga-

* Corresponding author. Phone: (0)6 249 2927; fax: (0)6 249 0760; e-mail: Mark.Humphrey@anu.edu.au.

[1] For Part IV, see Ref. [1].

PII S0022-328X(96)06197-9

Scheme: R = H (1), NO_2 (2), $C_6H_4NO_2$-4 (3), $CH{=}CHC_6H_4NO_2$-4,(*E*) (4).

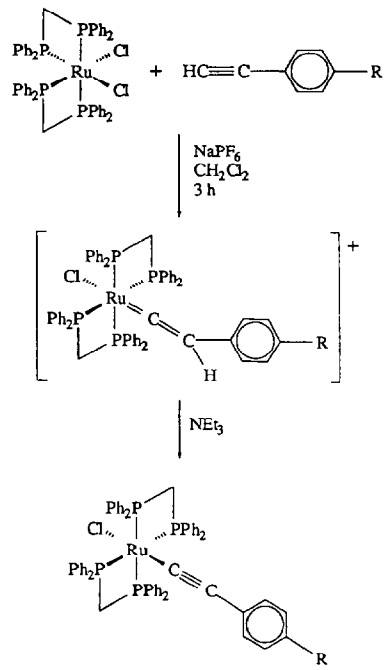

Scheme 1. R = H (1), NO_2 (2), $C_6H_4NO_2$-4 (3), $CH{=}CHC_6H_4NO_2$-4, (*E*) (4).

tions of molecular non-linearities to octahedral ruthenium σ-acetylide complexes of general formula *trans*-$[Ru(C{\equiv}CC_6H_4R\text{-}4)Cl(dppm)_2]$ (R = H, NO_2, $C_6H_4NO_2$-4, $CH{=}CHC_6H_4NO_2$-4,(*E*)); the results of these studies are detailed below.

2. Results and discussion

2.1. Syntheses and spectroscopic characterization

The synthetic method employed was analogous to that previously used by Touchard et al. [15] and is summarized in Scheme 1; complex **1** was described in this earlier report [15] and complex **2** in a paper which appeared while the current studies were underway [14].

The new complexes have similar spectral properties to the previously reported octahedral ruthenium σ-acetylides. Thus, the IR spectra contain characteristic $\nu(C{\equiv}C)$ at 2067 (**3**) and 2065 (**4**) cm^{-1}, between those of **1** (2075 cm^{-1}) and **2** (2045 cm^{-1}); the C≡C bond order is decreased as electron density is drawn to the nitro group, an effect less marked in **3** and **4** than in **2** owing to the more remote electron withdrawing substituent. The ^{31}P NMR spectra contain singlets at −5.7 (**3**) and −5.8 (**4**) ppm, consistent with trans-disposed ligands. The FAB mass spectra of both **3** and **4** contain signals corresponding to the molecular ion, with fragment ions due to competitive loss of chloro and acetylide ligands. Although the molecular composition of both **3** and **4** could be established from spectral data, a single crystal X-ray structural study of **3** was carried out to (i) afford accurate bond length data about the metal–acetylide linkage, (ii) give solid-state packing informa-

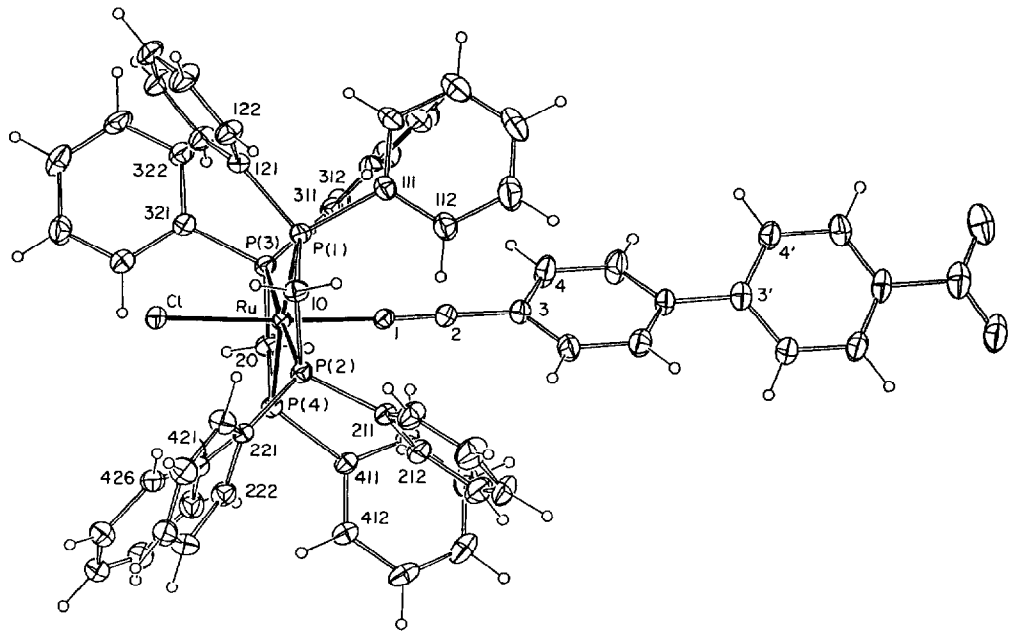

Fig. 1. Molecular geometry and atomic labelling scheme for *trans*-$[Ru(C{\equiv}CC_6H_4C_6H_4NO_2\text{-}4,4')Cl(dppm)_2]$ (**3**). 20% thermal ellipsoids are shown for the non-hydrogen atoms; hydrogen atoms have arbitrary radii of 0.1 Å.

Table 1
Atomic coordinates and equivalent isotropic thermal parameters for the non-hydrogen atoms in *trans*-[Ru(C≡$CC_6H_4C_6H_4NO_2$-4,4′)Cl(dppm)$_2$] (**3**)

Atom	*x*	*y*	*z*	U_{eq} (Å^2)
Ru	0.33150(2)	0.50445(4)	0.63696(1)	0.0353(1)
Cl	0.37866(7)	0.4544(1)	0.71740(4)	0.0517(5)
C(1)	0.2857(2)	0.5431(4)	0.5750(2)	0.041(2)
C(2)	0.2566(3)	0.5639(4)	0.5380(2)	0.051(2)
C(3)	0.2209(3)	0.5902(4)	0.4941(2)	0.051(2)
C(4)	0.2223(3)	0.5113(5)	0.4568(2)	0.076(2)
C(5)	0.1875(3)	0.5352(5)	0.4141(2)	0.080(3)
C(6)	0.1506(3)	0.6361(5)	0.4075(2)	0.054(2)
C(7)	0.1501(3)	0.7155(5)	0.4436(2)	0.069(2)
C(8)	0.1849(3)	0.6930(5)	0.4864(2)	0.070(2)
C(3′)	0.1131(3)	0.6592(5)	0.3621(2)	0.058(2)
C(4′)	0.0826(3)	0.5698(5)	0.3363(2)	0.067(2)
C(5′)	0.0498(3)	0.5903(5)	0.2926(2)	0.072(2)
C(6′)	0.0475(3)	0.7009(5)	0.2761(2)	0.065(2)
N(6′)	0.0157(2)	0.7199(5)	0.2286(1)	0.080(2)
O(61′)	−0.0114(2)	0.6367(4)	0.2081(1)	0.103(2)
O(62′)	0.0199(2)	0.8191(4)	0.2120(1)	0.104(2)
C(7′)	0.0743(3)	0.7932(5)	0.3007(2)	0.070(2)
C(8′)	0.1074(3)	0.7710(5)	0.3436(2)	0.065(2)
P(1)	0.22197(7)	0.4349(1)	0.66384(4)	0.0399(4)
C(111)	0.1440(2)	0.4198(4)	0.6249(2)	0.049(2)
C(112)	0.1182(3)	0.5169(5)	0.6009(2)	0.067(2)
C(113)	0.0624(3)	0.5057(6)	0.5688(2)	0.088(3)
C(114)	0.0343(3)	0.3982(7)	0.5599(2)	0.093(3)
C(115)	0.0583(3)	0.3032(6)	0.5833(2)	0.085(3)
C(116)	0.1136(3)	0.3133(5)	0.6160(2)	0.063(2)
C(121)	0.2145(2)	0.3060(4)	0.7011(2)	0.043(2)
C(122)	0.1621(3)	0.2948(5)	0.7342(2)	0.064(2)
C(123)	0.1564(3)	0.1924(5)	0.7598(2)	0.076(3)
C(124)	0.2018(3)	0.1019(5)	0.7513(2)	0.073(2)
C(125)	0.2536(3)	0.1127(5)	0.7192(2)	0.071(2)
C(126)	0.2609(3)	0.2162(4)	0.6943(2)	0.055(2)
C(10)	0.2030(3)	0.5638(4)	0.7001(2)	0.047(2)
P(2)	0.27297(7)	0.6576(1)	0.67594(4)	0.0405(4)
C(211)	0.2305(3)	0.7764(4)	0.6433(2)	0.046(2)
C(212)	0.2629(3)	0.8194(4)	0.6037(2)	0.054(2)
C(213)	0.2359(3)	0.9175(5)	0.5811(2)	0.070(2)
C(214)	0.1773(3)	0.9715(5)	0.5976(2)	0.081(3)
C(215)	0.1445(3)	0.9301(5)	0.6370(2)	0.090(3)
C(216)	0.1713(3)	0.8330(5)	0.6601(2)	0.068(2)
C(221)	0.3064(2)	0.7422(4)	0.7268(2)	0.040(2)
C(222)	0.3690(3)	0.8007(4)	0.7226(2)	0.053(2)
C(223)	0.3929(3)	0.8745(5)	0.7585(2)	0.068(2)
C(224)	0.3534(3)	0.8876(5)	0.7988(2)	0.064(2)
C(225)	0.2916(3)	0.8282(5)	0.8033(2)	0.063(2)
C(226)	0.2674(3)	0.7556(5)	0.7676(2)	0.057(2)
P(3)	0.38480(7)	0.3509(1)	0.59718(4)	0.0404(4)
C(311)	0.3419(3)	0.2784(4)	0.5471(2)	0.045(2)
C(312)	0.3815(3)	0.2296(4)	0.5114(2)	0.054(2)
C(313)	0.3480(3)	0.1702(5)	0.4749(2)	0.067(2)
C(314)	0.2755(3)	0.1587(5)	0.4742(2)	0.070(2)
C(315)	0.2352(3)	0.2066(5)	0.5098(2)	0.068(2)
C(316)	0.2688(3)	0.2679(5)	0.5460(2)	0.056(2)
C(321)	0.4284(3)	0.2292(4)	0.6269(2)	0.044(2)
C(322)	0.4010(3)	0.1186(4)	0.6239(2)	0.053(2)
C(323)	0.4334(3)	0.0270(4)	0.6483(2)	0.071(2)
C(324)	0.4929(3)	0.0461(5)	0.6753(2)	0.077(3)
C(325)	0.5202(3)	0.1551(5)	0.6789(2)	0.073(2)
C(326)	0.4878(3)	0.2478(5)	0.6557(2)	0.062(2)
C(20)	0.4579(3)	0.4378(4)	0.5727(2)	0.050(2)
P(4)	0.43750(7)	0.5734(1)	0.60362(4)	0.0410(4)

Table 1 (continued)

Atom	*x*	*y*	*z*	U_{eq} (Å^2)
C(411)	0.4352(2)	0.6850(4)	0.5574(2)	0.043(2)
C(412)	0.4553(3)	0.7985(4)	0.5680(2)	0.054(2)
C(413)	0.4464(3)	0.8865(4)	0.5354(2)	0.071(2)
C(414)	0.4193(3)	0.8609(5)	0.4914(2)	0.080(3)
C(415)	0.4004(3)	0.7506(5)	0.4795(2)	0.068(2)
C(416)	0.4075(3)	0.6625(4)	0.5125(2)	0.054(2)
C(421)	0.5192(2)	0.6137(4)	0.6352(2)	0.046(2)
C(422)	0.5824(3)	0.6268(5)	0.6116(2)	0.062(2)
C(423)	0.6421(3)	0.6696(5)	0.6347(2)	0.073(2)
C(424)	0.6386(3)	0.7002(5)	0.6815(2)	0.076(2)
C(425)	0.5772(3)	0.6865(5)	0.7056(2)	0.070(2)
C(426)	0.5167(3)	0.6418(4)	0.6830(2)	0.053(2)
Cl(1)	0.2230(1)	0.4402(2)	0.83315(8)	0.132(1)
Cl(2)	0.3066(2)	0.5925(2)	0.88790(8)	0.169(1)
C(0)	0.3054(4)	0.5008(6)	0.8411(3)	0.117(4)
Cl(1′) [a]	−0.0617(5)	0.9692(6)	0.5722(4)	0.340(7)
Cl(2′) [a]	−0.0932(3)	0.7322(5)	0.5819(2)	0.196(3)
C(0′) [a,b]	−0.0394(9)	0.840(2)	0.5937(6)	0.155(7)
Cl(1″) [a,b]	−0.0261(6)	0.941(1)	0.5422(4)	0.395(6)
Cl(2″) [a,b]	−0.057(1)	0.772(2)	0.5795(7)	0.72(1)
C(0″) [a,b]	0.001(1)	0.831(2)	0.5414(7)	0.178(8)

[a] Site occupancy factor = 0.5. [b] Isotropic thermal parameter.

tion, and (iii) generate accurate atomic coordinates as input data for the semi-empirical calculations detailed below.

2.2. X-ray structural study of *trans*-[Ru(C≡$CC_6H_4C_6H_4NO_2$-4,4′)Cl(dppm)$_2$] (3)

The solid state structure of **3** is shown in Fig. 1. Atomic coordinates are listed in Table 1 and selected bond lengths and angles are given in Table 2; the latter table also includes relevant data from cognate structural determinations.

The structural study confirms the octahedral geometry at ruthenium and trans-disposed chloro and acetylide ligands. Important bond lengths and angles are similar to those of the structurally characterized analogues *trans*-[Ru(C≡$CC_6H_4NO_2$-4)Cl(dppm)$_2$] (**2**) [14] and *trans*-[Ru(C≡CPh)Cl(dppe)$_2$] (**5**) [13]; clearly, the strong acceptor nitro group has little effect on acetylide geometry in the ground state structure of these complexes. Comparison with the related *trans*-[Ru(C≡CH)-Cl(dppm)$_2$] (**6**) [15,18] is less clear; the acetylide ligand is a much stronger π-donor than the arylacetylide lig-

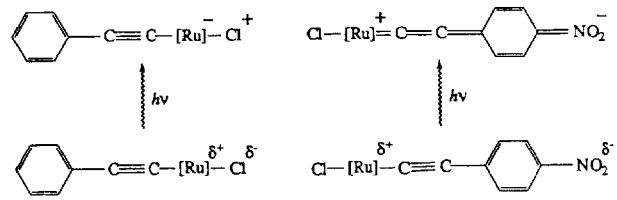

Fig. 2. Ground and excited state dipoles for LMCT in **1** (left) and MLCT in **2** (right); [Ru] ≡ *trans*-Ru(dppm)$_2$.

Table 2
Selected bond lengths (Å) and angles (deg) for *trans*-[Ru(C≡$CC_6H_4C_6H_4NO_2$-4,4′)Cl(dppm)$_2$] (**3**) and related complexes

	2 [a]	**3** [b]	**5** [c]	**6** [d]
Ru–Cl	2.483(2)	2.499(1)	2.479(1)	2.628(2)
Ru–P(1)	2.379(2)	2.350(1)	2.352(1)	2.354(1)
Ru–P(2)	2.358(2)	2.361(1)	2.368(1)	2.318(1)
Ru–P(3)	2.332(2)	2.330(1)	2.373(1)	2.354(1)
Ru–P(4)	2.332(2)	2.358(1)	2.392(1)	2.318(1)
Ru–C(1)	1.998(7)	1.994(4)	2.007(5)	1.906(9)
C(1)–C(2)	1.190(8)	1.198(6)	1.198(7)	1.162(9)
C(2)–C(3)	1.428(8)	1.439(7)	1.445(8)	—
Cl–Ru–C(1)	177.7(2)	175.2(1)	175.7(1)	178.3(8)
Ru–C(1)–C(2)	176.8(5)	177.9(4)	174.1(5)	177.0(6)
C(1)–C(2)–C(3)	168.4(7)	179.1(5)	— [e]	—

[a] Ref. [14]. [b] This work. [c] **5** ≡ *trans*-[Ru(C≡CPh)Cl(dppe)$_2$], Ref. [13]. [d] **6** ≡ *trans*-[Ru(C≡CH)Cl(dppm)$_2$], Refs. [15,18]. [e] Not reported.

ands in **2**, **3** and **5**. For the arylacetylide complexes, however, Ru–C distances in particular seem insensitive to structural variation, an important factor when combining molecular fragments for the semi-empirical calculations described below. For **3**, distances and angles within the phosphine and acetylide ligands are not unusual. Interestingly, the phenyl rings of the acetylide ligand are not coplanar, with a dihedral angle of 33°.

While the focus of our investigations is the molecular optical non-linearities of these acetylide complexes, it was also of interest to examine crystal packing as an indicator of bulk material response. The centrosymmetric arrangement in the lattice ensures that no bulk response would be observed, and suggests that consideration needs to be given to crystal engineering, to translate molecular non-linearities into enhanced bulk susceptibilities.

2.3. Semi-empirical calculations

Quadratic optical non-linearities of the systematically-varied series of complexes, evaluated using ZINDO, are given in Table 3; molecular geometries are taken from crystallographically-obtained atomic coordinates with the exceptions of **1** and **4**, where crystallographically-obtained molecular fragments were combined assuming a Ru–C(acetylide) distance of 1.99 Å (from the data in Table 2, this seems a valid assumption).

Not surprisingly, the centrosymmetric molecule *trans*-[$RuCl_2$(dppm)$_2$] has a β value of zero. Its isomer, *cis*-[$RuCl_2$(dppm)$_2$], with a non-zero dipole moment, has a non-zero first hyperpolarizability; it is negative because β_{vec} is opposite in direction to the ground state dipole vector. Replacement of chloro in *trans*-[$RuCl_2$(dppm)$_2$] by phenylacetylide to give **1** also removes the centre of symmetry and affords a non-zero β_{vec} value. Substituting the aryl 4-H in **1** by 4-NO_2 to afford **2** leads to an increase in non-linearity and reversal in sign. The latter can be understood by considering the ground and excited state dipoles of **1** and **2** for the important LMCT (**1**) and MLCT (**2**) transitions (Fig. 2). The LMCT in **1** gives rise to a change in dipole direction between ground and excited states, and a corresponding negative quadratic hyperpolarizability, whereas the MLCT in **2** (arising from the presence of the strong acceptor substituent) results in no change in dipole direction between ground and excited states, and a positive β_{vec}.

Chain-lengthening, in replacing the 4-nitrophenylacetylide ligand in **2** by a 4,4′-nitrobiphenylacetylide ligand to give **3** leads (not surprisingly) to an increase in non-linearity. A further increase in β_{vec} is found on replacing the biphenylene unit in **3** by an (*E*)-stilbenyl group to give **4**.

The phenylene groups in the nitrostilbenylacetylide ligand in **4** are close to coplanarity (dihedral angle =

Table 3
Calculated β_{vec} (10^{-30} cm^5 esu^{-1}; $\hbar\omega$ = 0.65 eV)

Complex	β_{vec}
trans-[$RuCl_2$(dppm)$_2$]	0
cis-[$RuCl_2$(dppm)$_2$]	−8
trans-[Ru(C≡CPh)Cl(dppm)$_2$] (**1**)	−13
trans-[Ru(C≡$CC_6H_4NO_2$-4)Cl(dppm)$_2$] (**2**)	34
trans-[Ru(C≡$CC_6H_4C_6H_4NO_2$-4,4′)Cl(dppm)$_2$] (**3**)	45
trans-[Ru(C≡CC_6H_4CH=$CHC_6H_4NO_2$-4,4′,(*E*))Cl(dppm)$_2$] (**4**)	60

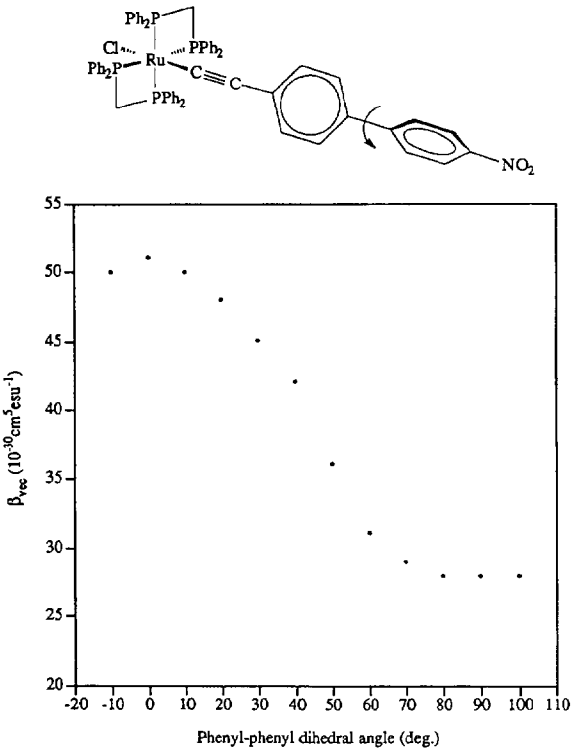

Fig. 3. Effect of varying the phenylene–phenylene dihedral angle from the crystallographically-determined value of 33° on the calculated hyperpolarizability for *trans*-[Ru(C≡CC$_6$H$_4$C$_6$H$_4$NO$_2$-4,4′)Cl(dppm)$_2$] (**3**).

12.5°, fragment from [Ru(C≡CC$_6$H$_4$CH=CHC$_6$H$_4$-NO$_2$-4,4′,(*E*))(PPh$_3$)$_2$(η-C$_5$H$_5$)] [19]); as mentioned above, this is not true for the phenylene units in the nitrobiphenylacetylide ligand in **3**. We have previously reported the effect of nitrophenyl group rotation with respect to the ligated metal centre in [Ru(C≡CC$_6$H$_4$-NO$_2$-4)(PMe$_3$)$_2$(η-C$_5$H$_5$)], where a 20% variation in response was noted [8]. We have now examined the significance of coplanarity of the phenylene groups in the nitrobiphenylacetylide ligand in **3** (Fig. 3), where a dihedral angle of 0° corresponds to coplanarity and 90° to orthogonality of the phenylene rings. For **3**, a variation of about 50% is apparent between maximum (coplanarity) and minimum (orthogonality) responses, indicating that this structural factor is more important for optimizing non-linear optical response than orientation of the ring adjacent to the acetylide.

3. Conclusion

The systematically-varied series of complexes considered above allows several conclusions to be made about molecular quadratic optical non-linearity in metal acetylides. The presence of a strong acceptor group (–NO$_2$) leads to a marked increase in computed non-linearity. Chromophore chain-lengthening results in enhanced calculated non-linear optical response. The smaller non-linearity for the biphenylene-containing complex **3** compared with the stilbenylacetylide complex **4**, coupled to the difficulty in enforcing coplanarity in the former, and the sharp decrease in response when rings are not oriented most favourably, suggests that ene-linkage between phenylene rings is the most effective for constructing efficient metal acetylide chromophores for non-linear optical responses. Further studies with systematically-varied complexes are currently underway.

4. Experimental details

4.1. General conditions

All reactions were performed under a nitrogen atmosphere with the use of Schlenk techniques unless otherwise stated. CH_2Cl_2 was dried by distilling over CaH_2; other solvents were used as-received. Column chromatography was performed using Merck aluminium oxide 90 active basic (activity stage II, 70–230 mesh ASTM). 'Pet. spirit' refers to a fraction of petroleum ether of boiling range 60–80°C.

4.2. Instruments

Mass spectra were recorded using a VG ZAB 2SEQ instrument (30 kV Cs^+ ions, current 1 mA, accelerating potential 8 kV, 3-nitrobenzyl alcohol matrix) at the Research School of Chemistry, Australian National University; peaks are reported as m/z (assignment, relative intensity). Microanalyses were carried out at the Research School of Chemistry, Australian National University. Infrared spectra were recorded as KBr pellets using a Perkin–Elmer 1600 FT-IR or a Perkin–Elmer System 2000 FT-IR.

^{1}H, ^{13}C and ^{31}P NMR spectra were recorded using a Varian Gemini-300 FT NMR spectrometer and are referenced to residual $CHCl_3$ (7.24 ppm), $CDCl_3$ (77.0 ppm) or external 85% H_3PO_4 (0.0 ppm) respectively. Spectral assignments follow the numbering scheme shown in Fig. 4.

4.3. Starting materials

The following were prepared by literature methods: *cis*-[RuCl$_2$(dppm)$_2$] [20], 4-ethynylnitrobenzene [21],

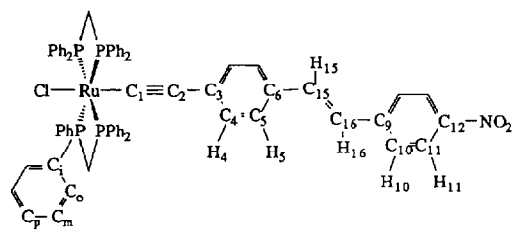

Fig. 4. Numbering scheme used in spectral assignments.

4,4′-$HC{\equiv}CC_6H_4C_6H_4NO_2$ [22], (*E*),4,4′-$HC{\equiv}CC_6H_4CH{=}CHC_6H_4NO_2$ [19]. Phenylacetylene and dppm (Aldrich) were used as-received.

4.4. Preparation of σ-acetylide complexes

4.4.1. *trans*-[Ru(C≡CPh)Cl(dppm)$_2$] (1)

A mixture of *cis*-[$RuCl_2$(dppm)$_2$] (400 mg, 0.43 mmol), phenylacetylene (94 μl, 0.85 mmol) and $NaPF_6$ (140 mg, 0.85 mmol) was stirred in CH_2Cl_2 (10 ml) for 3 h at room temperature. Two equivalents of NEt_3 were added to deprotonate the vinylidene complex formed. The product was immediately adsorbed onto alumina by adding the alumina to the solution and removing the solvent under vacuum. It was placed on a short chromatography column. Elution with 20% CH_2Cl_2–pet. spirit removed excess acetylene. Subsequent elution with 60% CH_2Cl_2–pet. spirit removed the product. The product was precipitated by removing the CH_2Cl_2 on a rotary evaporator. Upon filtering, 260 mg of yellow powder was isolated (61%) and its identity confirmed by comparison of spectral data with those in the literature [15]. IR (KBr): ν(C≡C) 2075 cm^{-1}. ^1H NMR: (δ, 300 MHz, $CDCl_3$); 8.84 (m, 3H, H_5 and H_6), 7.45 to 7.02 (40H, Ph), 6.08 (d, J_{HH} = 7 Hz, 2H, H_4), 4.89 (m, 4H, CH_2). ^{31}P NMR: (δ, 121 MHz, $CDCl_3$); −5.5 (PPh_2).

4.4.2. *trans*-[Ru(C≡$CC_6H_4NO_2$-4)Cl(dppm)$_2$] (2)

Following the method above, *cis*-[$RuCl_2$(dppm)$_2$] (400 mg, 0.43 mmol), 4-$HC{\equiv}CC_6H_4NO_2$ (125 mg, 0.85 mmol) and $NaPF_6$ (140 mg, 0.85 mmol) afforded 345 mg of red powder (71%). Anal. Found: C, 66.45; H, 4.87; N, 1.33. $C_{58}H_{48}ClNO_2P_4Ru$. Calc.: C, 66.26; H, 4.60; N, 1.33%. IR (KBr): ν(C≡C) 2045 cm^{-1}. ^1H NMR: (δ, 300 MHz, $CDCl_3$); 7.72 (d, J_{HH} = 9 Hz, 2H, H_5), 7.43 to 7.03 (40H, Ph), 5.89 (d, J_{HH} = 9 Hz, 2H, H_4), 4.90 (m, 4H, CH_2). ^{13}C NMR: (δ, 75 MHz, $CDCl_3$); 141.9 (C_6), 137.6 (C_3), 134.5 ($C_{i,m}$), 133.6 (C_o partially obscuring C_i), 133.2 (C_o), 129.8 (C_4), 129.5 (C_p), 129.3 (C_p), 127.6 (C_m), 122.9 (C_5), 115.8 (C_2), 50.2 (CH_2). ^{31}P NMR: (δ, 121 MHz, $CDCl_3$); −6.1 (PPh_2). Complex (**2**) has been reported elsewhere [14].

4.4.3. *trans*-[Ru(C≡$CC_6H_4C_6H_4NO_2$-4,4′)Cl(dppm)$_2$] (3)

Following the method above, *cis*-[$RuCl_2$(dppm)$_2$] (370 mg, 0.39 mmol), 4,4′-$HC{\equiv}CC_6H_4C_6H_4NO_2$ (175 mg, 0.78 mmol) and $NaPF_6$ (135 mg, 0.80 mmol) afforded 260 mg of deep red powder (59%). FAB MS: 1282 ([M + matrix]$^+$, 5), 1127 ([M]$^+$, 60), 1092 ([M − Cl]$^+$, 27), 869 ([Ru(dppm)$_2$]$^+$, 34). Anal. Found: C, 68.02; H, 4.66; N, 1.20. $C_{64}H_{52}ClNO_2P_4Ru$. Calc.: C, 68.18; H, 4.65; N, 1.24%. IR (KBr): ν(C≡C) 2067 cm^{-1}. ^1H NMR: (δ, 300 MHz, $CDCl_3$); 8.22 (d, J_{HH} = 9 Hz, 2H, H_{11}), 7.65 (d, J_{HH} = 9 Hz, 2H, H_{10}), 7.44 to 7.05 (42H, Ph), 6.12 (d, J_{HH} = 8 Hz, 2H, H_4), 4.90 (m, 4H, CH_2). ^{13}C NMR: (δ, 75 MHz, $CDCl_3$); 147.8 (C_{12}), 146.0 (C_9), 135.0 ($C_{i,m}$), 134.0 ($C_{i,m}$), 133.6 (C_o), 133.3 (C_o), 131.7, 131.5 (C_3 and C_6), 130.7 (C_4), 129.3 (C_p), 129.1 (C_p), 127.5 (C_p), 126.5, 125.8 (C_5 and C_{10}), 124.0 (C_{11}), 112.9 (C_2), 50.3 (CH_2). ^{31}P NMR: (δ, 121 MHz, $CDCl_3$); −5.7 (PPh_2). A crystal suitable for X-ray diffraction study was grown from CH_2Cl_2–hexane.

4.4.4. *trans*-[Ru(C≡$CC_6H_4CH{=}CHC_6H_4NO_2$-4,4′,(*E*))Cl(dppm)$_2$] (4)

Following the method above, *cis*-[$RuCl_2$(dppm)$_2$] (400 mg, 0.43 mmol), (*E*),4,4′-$HC{\equiv}CC_6H_4CH{=}CHC_6H_4NO_2$ (200 mg, 0.80 mmol) and $NaPF_6$ (145 mg, 0.86 mmol) afforded 260 mg of dark red powder (53%). FAB MS: 1153 ([M]$^+$, 95), 929 ([(dppm)$_2$ClRuC≡C]$^+$, 16), 869 ([Ru(dppm)$_2$]$^+$, 41). Anal. Found: C, 68.10; H, 4.55; N, 1.20. $C_{66}H_{54}ClNO_2P_4Ru$. Calc.: C, 68.72; H, 4.72; N, 1.21%. IR (KBr): ν(C≡C) 2065 cm^{-1}. ^1H NMR: (δ, 300 MHz, $CDCl_3$); 8.17 (d, J_{HH} = 9 Hz, 2H, H_{11}), 7.55 to 7.04 (45H, Ph partially obscuring H_{16}), 6.93 (d, J_{HH} = 15 Hz, 1H, H_{15}), 6.03 (d, J_{HH} = 8 Hz, 2H, H_4), 4.90 (m, 4H, CH_2). ^{13}C NMR: (δ, 75 MHz, $CDCl_3$); 146.0 (C_{12}), 144.7 (C_9), 135.0 (C_i), 134.0 ($C_{i,m}$), 133.9 (C_{16}), 133.7 (C_o partially obscuring C_i), 133.3 (C_o), 131.8 (C_3), 130.5 (C_4), 129.9 (C_6), 129.3 (C_p), 129.1 (C_p), 127.5 (C_p), 126.2, 125.9 (C_5 and C_{10}), 124.2 (C_{11}), 123.1 (C_{15}), 113.9 (C_2), 50.3 (CH_2). ^{31}P NMR: (δ, 121 MHz, $CDCl_3$); −5.8 (PPh_2).

4.5. X-ray structure determination

4.5.1. General conditions

A unique room temperature diffractometer data set ($T \approx 295$ K; monochromatic Mo Kα radiation (λ = 0.7107$_3$ Å; 2θ–θ scan mode, $2\theta_{max}$ 50°) was obtained, yielding 10318 independent reflections, 6596 of these with $I \geq 3\sigma(I)$ being considered 'observed' and used in the full-matrix least-squares refinement after Gaussian absorption correction. Anisotropic thermal parameters were refined for the non-hydrogen atoms, with the exception of solvent″ and C(0′) which were refined isotropically; (x, y, z, U_{iso})$_H$ were included constrained at estimated values. Difference map artefacts were modelled acceptably as two molecules of dichloromethane of solvation, one of which is disordered over two positions (′ and ″) with site occupancy factors 0.5 each following refinement. Conventional residuals R, R_w on $|F|$ at convergence were 0.044, 0.046, statistical reflection weights derivative of $\sigma^2(I) = \sigma^2(I_{diff}) + \sigma^4 0.0004(I_{diff})$ being used. Computation used the XTAL 3.2 program system implemented by Hall [23]. Pertinent results are given in Fig. 1 and Tables 1 and 2. Tables of hydrogen atom coordinates

and thermal parameters and a complete list of bond lengths and angles for non-hydrogen atoms have been deposited at the Cambridge Crystallographic Data Centre.

4.5.2. Crystal data

$C_{64}H_{52}ClNO_2P_4Ru \cdot 2CH_2Cl_2$, $M = 1297.4$. Monoclinic, space group $P2_1/c$ (No. 14), $a = 18.843(4)$, $b = 11.508(3)$, $c = 28.301(6)$ Å, $\beta = 90.81(2)°$, $V = 6136(2)$ Å^3. ($Z = 4$) $D_c = 1.404$ g cm^{-3}; $F(000) = 2656$. $\mu_{Mo} = 6.2$ cm^{-1}; specimen: $0.23 \times 0.35 \times 0.43$ mm^3; $A_{min,max} = 1.13, 1.25$.

4.6. Computational details

Results were obtained using ZINDO (June 1994 version) from Biosym Technologies, San Diego, CA, USA [24], implemented on a Silicon Graphics INDY workstation without parameter manipulation or basis function alteration. The input for calculations were the atomic coordinates obtained from X-ray diffraction structural determinations except in the cases of **1** and **4**, where coordinates were produced from a combination of fragments of related structurally characterized complexes ([RuCl(C≡CPh)(dppe)$_2$] [13], [RuCl(C≡CC$_6$H$_4$NO$_2$-4)(dppm)$_2$] [14] and [Ru(C≡CC$_6$H$_4$CH=CHC$_6$H$_4$NO$_2$-4,4′,(*E*))(PPh$_3$)$_2$(η-C$_5$H$_5$)] [19]) using the 'builder' routine in the molecular modelling package Insight II; Ru–C distances of 1.99 Å were assumed. CI calculations included single excitations; basis set sizes were increased progressively for all calculations until convergence ($\pm 2 \times 10^{-30}$ cm^5 esu^{-1}) in the computed β_{vec} value was reached (150–250 excited configurations).

Acknowledgments

We thank the Australian Research Council and Telstra for support of this work and Johnson-Matthey Technology Centre for a generous loan of ruthenium salts. IRW is the recipient of an Australian Postgraduate Research Award (Industry) and MGH holds an ARC Australian Research Fellowship.

References

[1] I.R. Whittall, M.G. Humphrey, M. Samoc, J. Swiatkiewicz and B. Luther-Davies, *Organometallics, 14* (1995) 5493.
[2] S.R. Marder, J.E. Sohn and G.D. Stucky (eds.), *Materials for Nonlinear Optics*, American Chemical Society, Washington, DC, 1991.
[3] H.S. Nalwa, *Appl. Organomet. Chem., 5* (1991) 349.
[4] N.J. Long, *Angew. Chem. Int. Ed. Engl., 34* (1995) 21.
[5] D.R. Kanis, M.A. Ratner and T.J. Marks, *J. Am. Chem. Soc., 112* (1990) 8203.
[6] D.R. Kanis, M.A. Ratner and T.J. Marks, *J. Am. Chem. Soc., 114* (1992) 10338.
[7] D.R. Kanis, M.A. Ratner, T.J. Marks and M.C. Zerner, *Chem. Mater., 3* (1991) 19.
[8] I.R. Whittall, M.G. Humphrey, D.C.R. Hockless, B.W. Skelton and A.H. White, *Organometallics, 14* (1995) 3970.
[9] C. Bianchini, P. Frediani, D. Masi, M. Peruzzini and F. Zanobini, *Organometallics, 13* (1994) 4616.
[10] T. Rappert and A. Yamamoto, *Organometallics, 13* (1994) 4984.
[11] Y. Sun, N.J. Taylor and A.J. Carty, *Organometallics, 11* (1992) 4293.
[12] S.J. Davies, B.F.G. Johnson, J. Lewis and P.R. Raithby, *J. Organomet. Chem., 414* (1991) C51.
[13] C.W. Faulkner, S.L. Ingham, M.S. Khan, J. Lewis, N.J. Long and P.R. Raithby, *Organometallics, 482* (1994) 139.
[14] A.J. Hodge, S.L. Ingham, A.K. Kakkar, M.S. Khan, J. Lewis, N.J. Long, D.G. Parker and P.R. Raithby, *J. Organomet. Chem., 488* (1995) 205.
[15] D. Touchard, P. Haquette, N. Pirio, L. Toupet and P.H. Dixneuf, *Organometallics, 12* (1993) 3132.
[16] M.S. Khan, A.K. Kakkar, S.L. Ingham, P.R. Raithby and J. Lewis, *J. Organomet. Chem., 472* (1994) 247.
[17] Z. Atherton, C.W. Faulkner, S.L. Ingham, A.K. Kakkar, M.S. Khan, J. Lewis, N.J. Long and P.R. Raithby, *J. Organomet. Chem., 462* (1993) 265.
[18] P. Haquette, N. Pirio, D. Touchard, L. Toupet and P.H. Dixneuf, *J. Chem. Soc. Chem. Commun.*, (1993) 163.
[19] I.R. Whittall, M.G. Humphrey, A. Persoons and S. Houbrechts, *Organometallics*, in press.
[20] B. Chaudret, G. Commenges and R. Poilblanc, *J. Chem. Soc. Dalton Trans.*, (1984) 1635.
[21] S. Takahashi, Y. Kuroyama, K. Sonogashira and N. Hagihara, *Synthesis*, (1980) 627.
[22] I.R. Whittall and M.G. Humphrey, in preparation.
[23] S.R. Hall, H.D. Flack and J.M. Stewart, *The* XTAL 3.2 *Reference Manual*, Universities of Western Australia, Geneva and Maryland, 1992.
[24] ZINDO *User Guide*, Biosym Technologies, San Diego, 1994.